93　8　31

Bias assisted microwave plasma
enhanced chemical vapor deposition
carbon nanoflake

Scanning electron microscopy, SEM

Transmission
electron microscopy, TEM

5 10
5nm

Abstract

Carbon based nano-materials including carbon nanotubes and carbon nanoflakes were directly grown on silicon wafers and carbon clothes by bias assisted microwave plasma enhanced chemical vapor deposition (MPCVD) as the electrode for proton exchange membrane fuel cell (PEMFC). The morphology and the structure of carbon based nano-materials were characterized by means of FESEM and HRTEM, respectively. The surface area of both carbon nanotubes based electrode and carbon nanoflakes based electrode were $90.31 m^2/g$ and $130.96 m^2/g$ from BET measurement. The dispersion of platinum catalysts was carried out by sputtering and chemical solution deposition methods. From HRTEM observation, the platinum particle size was less than 5nm from those two methods.

Keywords: bias assisted microwave plasma enhanced chemical vapor deposition, carbon nano-flakes, proton exchange membrane fuel cell

Introduction

In recent years, the proton exchange membrane fuel cell (PEMFC) used for space mission, terrestrial vehicle transportation, and local power generation has received increasing attention. Due to its high electrochemical performance efficiency, simple stack design, pollution-free, noise-free, and low temperature operation, PEMFC has become a promising candidate for portable power source. Besides, PEMFC with the promises such as the elimination of electrolyte leakage and lower corrosion has applications in the areas of military, aerospace and transportation. Emission product from PEMFC is free of environment-undesired gases, such as nitrogen oxide, carbon monoxide, carbon dioxide, and hydrocarbon, which are usually produced from internal combustion engines. Especially, carbon dioxide is absent in the reaction when the hydrogen is used as fuel [1].

PEMFC has incorporated various electrodes containing Pt / C. Due to cut the catalyst costs. Recently, lots of researchers have taken notice of new platinum supports for proton-exchange membrane fuel cell, such as carbon nanotubes [2-7] and carbon nanofibers [8] in order to reduce the utility of platinum catalyst. However, the conventional process was using carbon nanotubes powers mixed with solvent and inking on the carbon paper [2,9]. Directly growing high surface carbon based nanomaterials on the carbon paper and depositing Pt particle on these materials subsequently is necessary for the application of PEMFC.

In this study, we demonstrated an approach to synthesize carbon based nano-materials with high surface areas both on silicon substrates and carbon papers by adjusting the bias of MWPECVD system. We also successfully deposited the Pt catalyst with several nanometers on those nanomaterials by both chemical solution deposition methods and sputtering methods.

Experiment

Iron was first deposited on both the n-type (100) silicon wafer and the carbon cloth (E-tech.) respectively by e-beam evaporation and electroless plating as the catalyst for the growth of carbon based nano-materials. The reactive gas species are methane and hydrogen. The microwave power and the working pressure were set at 300W and 10Torr, respectively. The additive bias was adjusted from +200V to -200V. An optical pyrometer was used to monitor the substrate temperature. The carbon nanotubes were synthesized on the Fe-deposited substrates under the condition of applying negative bias from 0V to -200V during 20 minutes growth. On the other hand, the carbon nanowalls were grown under a successive process of applying 10 minutes negative bias and then 10 minute positive bias. For comparison, the deposition of platinum was carried out by means of electroless plating and sputtering. The solvents of electroless plating included glycol, PVP 4000, $PtCl_6$, and $RuCl_6$. The concentration of chemical solution was 0.01M. Moreover, the sputtering current was 10mA and the sputtering time was 30s. The characteristics of morphologies were achieved by means of scanning electron microscopy (Hitachi S4700I and JEOL 2500) after deposition. A high resolution transmission electro microscope (Philips Tecnai-20) was used to investigate the microstructure of carbon based nano-materials and the size of platinum particle. Structural characteristics were accomplished by Raman spectroscopy. The surface area measurement was relied on Brunauer Emmett Teller method (BET).

3

Results and Discussions

Carbon nanotubes could be obtained under a gas mixture of H_2/CH_4 with a ratio of 4/1 and 10Torr pressure on Fe(100A) deposited silicon substrate.Fig1 shows the SEM images of carbon nanotubes growth under various biases applied. Obviously, the length of carbon nanotubes was enhanced with increasing bias voltage. When the bias voltage increased, the tube became more aligned and sharp. Until the negative voltage reached -200V, the tube turned to tip-like .It was due to carbonaceous ion accelerated near to the substrate and accumulated, meanwhile H^+ etching sharpened the top of tube. It has been reported generally that applying negative bias could enhance the nucleation density of diamond. [10-12] In this experiment, the initial growing stage was the catalyst formed a carbon-sphered precursor and with the temperature raised, the tensile-forces induced the formation of short carbon nanotubes.

Electrostatic forces of the negative bias enhanced presented in the plasma drove the subsequent extension of the short carbon nanotubes to multiple-micron lengths. And, a key element to the mechanism proposed is defects in the carbon-sphered graphene-layers. Pentagon and heptagon rings are two types of defects found in graphene layers. Since the negative bias accelerated the growing rate of carbon nanotubes, defects on the tubes were accumulated more also. The basic tenets of the growth mechanism are as follows: Double [5-7] defects are in the equilibrium with the graphene layers in carbon nanotubes, via [6-6-6-6] to [5-7-7-5] Stone-Wales switches [13] .The [5-7] defects migrate thermally and at random. The [5-7] defects concentrated at the location that are energetically favorable and, which is the stem of a nanotube under tensile strain. The higher concentration of [5-7] defects in the stem increases the probability of interactions in [5-7] defects that result in [5-7-7-5] to [6-6-6-6] reverse Stone-Wales switches. The net migration of [5-7] defects to the stem, and the subsequent generation of hexagons in the stem, result in the lengthening of stem.
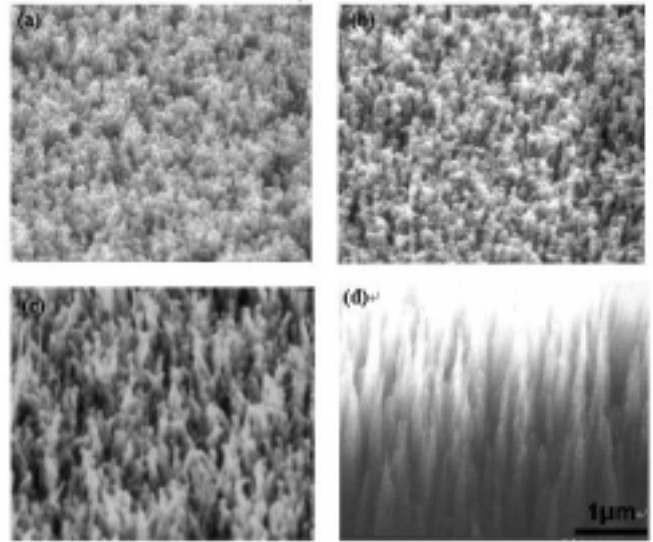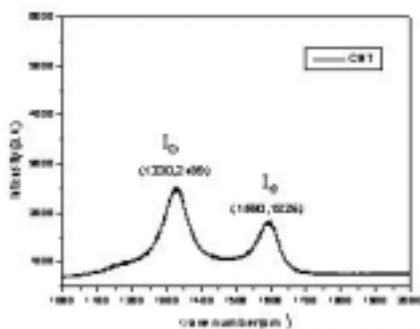

Figure 1

The HRTEM (Fig.2) shows the structure of muti-walled carbon nanotubes with hollow inside and the outer surrounded amorphous carbon.
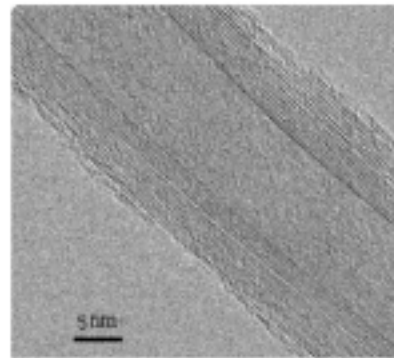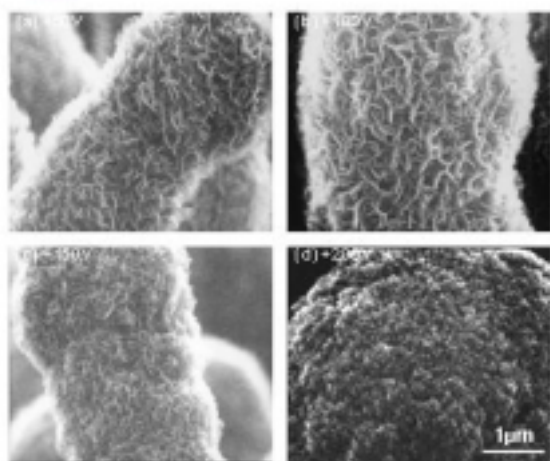

Figure 2

Raman spectrum (Fig.3) revealed that carbon nanotubes are characteristic of graphite. The first-order of Raman spectrum of carbon nanotube shows strong peaks at $1591cm^{-1}$(G line), which is high frequency E_2g first –order mode and $1348cm^{-1}$(roughly corresponding to the D-line associated with disorder-allowed zone –edge modes of graphite)
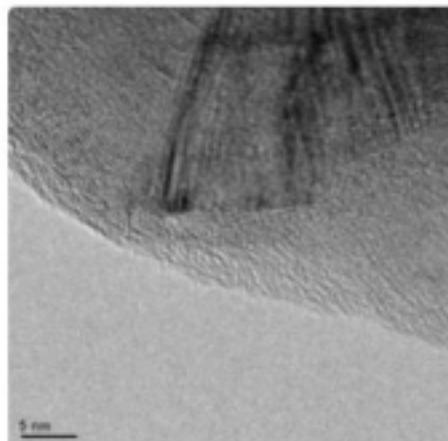
Figure 3

Fig.4 shows the SEM images of cross-sectional view of carbon nanoflakes. They were grown under various positive bias voltages adding after the negative bias applied each for 10 minutes. It reveals that along the stem body of the carbon nanotubes under the negative bias before, opposite ion bombardment and electrostatic force competing makes graphite sheets form a particular shape. With the positive bias voltage increasing, the pore formed of petaloid sheets became large until the competing forces lose the equilibrium.

The positive bias lead to another direction of net [5-7] migration since there exists the [5-7-7-5] to [6-6-6-6] reverse Stone-Wales switches under the negative bias applying. When the positive bias added, the carbon nanotubes had extended their lengths from the catalyst site which might be the secondary deposition. A special difference from published carbon nanoflakes is its 3-D structure. This could lift application of its high surface areas and chemical activity.

Figure 4

From the HRTEM images of Fig.5, a small-angle rotation existing between the basal plane layers of the petal due to weak interlayer (van der Waals) interaction in graphitic layer. The occurrence of interlayer rotation might be also a result of the difference in layer curvature.
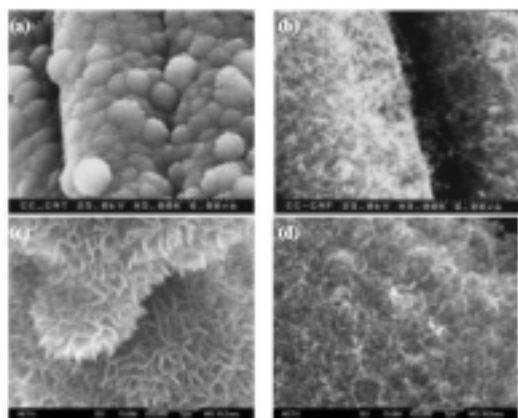

Figure 5

Fig 6 is the images of carbon nanotubes and carbon nanoflakes deposited on carbon cloth. The left image indicates that the porous structure is clear and uniform and between the fibers. However the carbon nanotubes on carbon cloth (right image) entangle with each other, lay down on the substrate and have random direction due to the round substrate so as the length limited even the negative bias can enhance it. We have another test to get the vertical carbon nanotubes, but if the density of carbon nanotubes isn't be controlled; the spraying of Pt particle may just deposit on the top surface. Therefore, even the carbon nanotubes make the smaller pore which still can't be utilized until the density is controlled. In additional, the vacancies between fibers couldn't be stuffed due to carbon nanotubes can't grow across the fiber so the left space wasted.

From the surface areas test by BET, the adsorption area of carbon cloth (15.02 m^2/g) obviously increased with the surface improvement by carbon nanotubes (90.31 m^2/g) and carbon nanoflakes (130.96 m^2/g). As prediction of porous structure make it more efficient, the carbon nanoflakes do

attribute to more surface areas than carbon nanotubes on carbon cloth.

Figure 6

The dispersion of platinum catalysts was carried out by sputtering and chemical solution deposition methods (poyol method). By sputtering Pt method, the working time just spend 20~60secs to get the Pt particles size range from 2~5nm. Fig.7 shows the TEM images of sputtering Pt on carbon nanotubes and carbon nanoflakes. Although the outcome on carbon nanotubes seems to be good, it isn't spray on every carbon nanotubes. However the Pt on carbon nanoflakes could be seen anywhere especially every petal on it. The reason can be traced to forward preparing carbon cloth experiment, the entangled morphology of carbon nanotubes leads to the property decay by sputtering Pt. Comparatively, the random extended carbon nanoflakes could collect Pt very well as long as they have the top-open structures.

About the chemical solution method, the preparing Pt/Ru mixing solution may need 1~2 hr, and this lead to different ratio of Pt/Ru. The solution were prepared by mixing PVP, Pt/Ru ions and ethylene glycol then put in hot chamber for reacting 1hr.We assume the ratio of Pt/Ru is 1:1. When we get the solution and immerse carbon nanotubes or carbon nanoflakes in it, it should be mixed with acetone to separate the Pt/Ru from other polymer and the dilute ration could affect the later alloy particle size. The separating procedure should be by centrifuge to make sure the pure Pt/Ru, but still has the impurity.

After this, ever immersed sample must dry in vacuum oven up to 200°C and this may cost 2 hr. From a succession of procedure, each part may affect the property of Pt/Ru on carbon nanotubes or carbon nanoflakes and hard to exam.
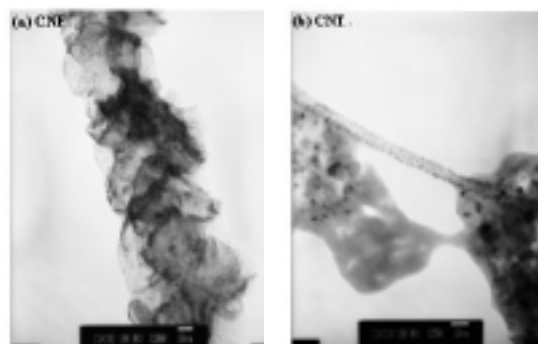
Figure 7

From Fig.8, we could determine the uniformity between sputtering and solution methods. The particles deposited by sputtering are separated well and the size is also well-controlled, besides each Pt has a single crystal structure by diffraction pattern identification. Otherwise the Pt/Ru on carbon nanoflakes by poyol isn't generally sprayed but has a twin specific line.
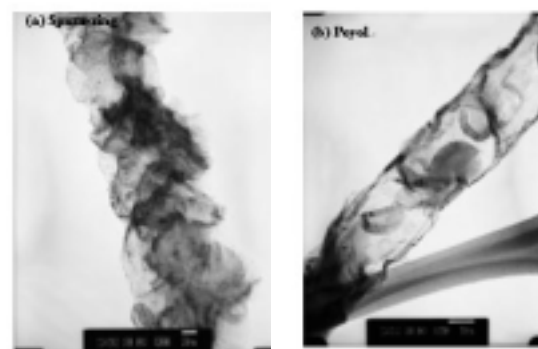
Figure 8

Reference
1. S. Srinivasan, O.A. Velev, A. Parthasarathy, D.J. Manko, A.J.Appleby, **J. Power Sources** 1991,36,299.
2. W. Li, C. Liang, J. Qiu, W. Zhou, H. Han, Z. Wei, G. Sun, Q. Xin, **Carbon** 2002,40,787
3. D. B. Buchholz, S. P. Doherty, R. P. H. Chang, **Carbon**,2003,41,1625.
4. B. Rajesh, V. Karthik, S. Karthikeyan, K Ravindranthan Thampi, J. M. Bonard, B. Viswanathan, **Fuel**, 2002, 81, 2177.

5. H. tang, J.H. Chen, Z.P.Huang, D.Z.Wang, Z.F.Ren, L. H. Nie, Y. F. Kuang, S.Z. Yao, **Carbon**, 2004, 42,191

6. H. Hou and Darrell H. Reneker, **Advanced Materials**, 2004,16, No.1,69.

7. C.Wang, M. Waje, X. Wang, J. M. Tang, Robert C. Haddon, Y. Yan, **Nano Letter**,2004,4,2,345.

8. C. A. Bessel, K. Lauberns, N. M. Rodriguez, R. Terry K. Baker, **The Journal of Physical Chemistry B**,2001,105,6,1115.

9. W. Z. Li, C. H. Liang, W. J. Zhou, J. S. Qiu, Z. H. Zhou, G. Q. Sun, J. Q. Xin, **The Journal of Physical Chemistry B**,2003,107,6292.

10. S. Yugo, T. Kanai, T. Kimura, and T. Muto, **Appl. Phys. Lett.** 58, 1036 (1991).

11. J. T. Huang, W. Y. Yeh, J. Hwang, and H. Chang, **Thin Solid Films** 315, 35 (1998).

12. R. Sto¨ckel, K. Janischowsky, S. Rohmfeld, J. Ristein, M. Hundhausen, and L. Ley, **Diamond Relat. Mater.** 5, 321 (1996)

13. By Chihiro Kuzuya, Wan In-Hwang, Shinji Hirako, Yukio Hishikawa, and Seiji Motojima, **Chem. Vap. Deposition 2002**, 8, No